JOURNAL OF OPTOELECTRONICS AND ADVANCED MATERIALS Vol. 10, No. 2, February 2008, p. 455 - 460

Phase equilibria investigation and characterization of the Au-In-Sb system

L. GOMIDŽELOVIĆ, D. ŽIVKOVIĆ[a*], N. TALIJAN[b], D. MANASIJEVIĆ[a], V. ĆOSOVIĆ[b], A. GRUJIĆ[b]
Mining and Metallurgy Institute, Zeleni bulevar 35, 19210 Bor, Serbia
[a]*University of Belgrade, Technical Faculty, VJ 12, 19210 Bor, Serbia*
[b]*Institute of Chemistry, Technology and Metallurgy, Njegoševa 12, 11000 Belgrade, Serbia*

The Au-In-Sb system is of great interest recently, because its alloys belong to the group of potential lead-free solder materials to be used in electronics, while as a part of Au-In-Sb-Te system, it presents a suitable phase change material in optical recording media. The results of phase equilibria investigation and characterization of the alloys in the AuIn-Sb section of the Au-In-Sb system are presented in this paper. The investigations were performed using different experimental methods – thermal analysis, optical microscopy and SEM-EDX, hardness and electrical conductivity measurements, and also, using ThermoCalc software based on adequate thermodynamic calculation.

(Received November 19, 2007; accepted February 7, 2008)

Keywords: Au-In-Sb system, phase equilibria, characterization

1. Introduction

Gold and gold alloys are widely applied in modern technical branches – electronics, communications, space and aero technologies, chemistry and medical science, etc. They are known for good mechanical and thermal properties, as well as corrosion consistency [1].

The Au-In-Sb system is of significant interest recently, because its alloys belong to the group of potential lead-free solder materials to be used in electronics [2], while as a part of Au-In-Sb-Te system, it presents a suitable phase change material in optical recording mediums [3,4].

The Au-In-Sb alloys are considered as a possible lead-free alternative to conventional Pb-bearing solders in step soldering, which are required for high density packaging of multi-chip modules demanding a number of solders with melting points over a wide temperature range [2]. Also, these alloys are important in the field of optical recording mediums to provide a medium able to cope with high recording density and a high transfer rate corresponding to the shortened wavelength and which is able to realize optimum direct overwrite without lowering the repetitive durability or storage stability of recorded signals [3]. In the optical disc of each of the above configurations, the recording layer is formed of a phase change material, e.g. Au-In-Sb-Te, which undergoes reversible phase changes on illumination by a light beam [4].

Therefore, mentioned gold-based system - ternary Au-In-Sb system, is the subject of different investigations and patents lately, for its phase diagram and characteristics are of importance in predicting the interface reactions between In-based solders and Au-substrate, as well as the interface reaction between layers in optical recording mediums, which can provide a tool for design a potential interface [2-4].

Phase equilibria of this system have been firstly studied by Kubiak and Schubert [5] and Tsai and Williams [6], during eighties. Based on these results, a compilation on the Au-In-Sb phase diagram determination has been done in the book "Phase Diagrams of Ternary Gold Alloys" of Prince and collaborators [7], while data on condensed phase equilibria in transition metal-In-Sb systems and predictions for thermally stable contacts to InSb is given in [8]. Recently, phase diagram of the Au-In-Sb system has been calculated using thermodynamic modeling and presented in literature by Liu et al. [9].

Having in mind this literature survey at one side, and latest demand for new lead-free gold-indium-based solders at the other side [10], the results of phase equilibria investigation and characterization of the AuIn-Sb section in the Au-In-Sb system are presented in this paper. The investigations were performed using different experimental methods – differential thermal analysis, optical microscopy, hardness and electrical conductivity measurements, aiming to contribute to the better knowledge of the investigated Au-In-Sb lead-free solder candidate.

2. Experimental

Investigated samples were chosen in the AuIn-Sb section of the Au-In-Sb system. The samples were prepared in an induction furnace under inert atmosphere, using metals - gold, indium and antimony of 99.99% purity. The composition and masses of chosen samples are given in Table 1.

Table 1. Composition and masses (in g) of the investigated samples.

Alloy	x_{Sb}	x_{Au}	x_{In}	m_{Sb}	m_{Au}	m_{In}
A1	0	0.5	0.5	0	3.8032	2.2145
A2	0.05	0.475	0.475	0.2304	3.5396	2.0623
A3	0.2	0.4	0.4	0.8693	2.8122	1.6386
A4	0.28	0.36	0.36	1.1813	2.4569	1.4317
A5	0.4	0.3	0.3	1.6169	1.9610	1.1429
A6	0.65	0.175	0.175	2.4158	1.0520	0.6129
A7	0.85	0.075	0.075	2.9678	0.4326	0.2468

DTA measurements have been carried out on the Derivatograph 1500 (MOM Budapest) apparatus under following conditions - air atmosphere, heating rate 10 ^oC/min, T_{max}=1073 K. As a referent material during measurements was used Al_2O_3. In order to test reproducibility of the results every measurement run was repeated, but no significant temperature deviation was found between the first series and repeated series of DTA measurements. The precision of the measurement in the investigated temperature interval was ±5 ^oC.

SEM-EDX analysis was performed on Philips microscope XL-300 type with EDX of resolution of 1 nm on 30 kV and 5 nm on 1 kV, extinction voltage of 0.2-30 kV and magnification of 2000x.

Microstructure analysis of investigated samples was performed by optic microscopy, using a Reichert MeF2 microscope (magnification x500). Solution of 1:1 HNO_3 was applied for structure development.

Electrical conductivity of investigated materials was measured using the standard apparatus -SIGMATEST 2.069 (Foerster) eddy current instrument for measurements of electrical conductivity of non-ferromagnetic metals based on complex impedance of the measuring probe with diameter of 8mm.

Hardness measurements were done using standard procedure according to Vickers.

3. Results and discussion

The results of the DTA heating measurements, including liquidus temperatures and other peak temperatures, are presented in Table 2.

Table 2. The results of DTA investigation.

Alloy	Composition, at%Sb	Temperature, ^oC	
		Liquidus	Other peak temperatures
A1	0	514	/
A2	5	490	418
A3	20	420	387
A4	28	377	359
A5	40	419	382
A6	60	524	384
A7	85	589	390

Based on starting thermodynamic data for the constitutive binary systems (given in Appendix), taken from COST531 Thermodynamic Database [11], thermodynamic modeling was done according to standard procedure [12]. Thermodynamic data for binary data are included in the COST 531 Database for Lead Free Solders [11], based on referent thermodynamic data for the Au–In system taken from [13], for the Au–Sb system published in [14], and thermodynamic data for the system In–Sb taken from [15].

The calculated phase diagram of the investigated AuIn-Sb section is presented in Fig.1, together with experimentally determined phase transition temperatures.

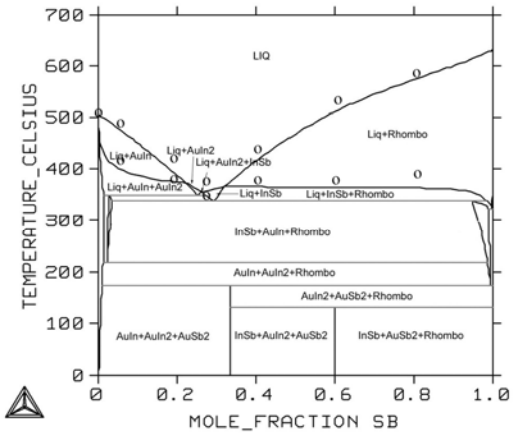

Fig.1. Calculated phase diagram of the AuIn-Sb section with experimental DTA points (circles)

It could be noticed that calculated phase diagram is in reasonable agreement with DTA measurements, approving experimentally the results of recent thermodynamic modeling presented in literature [9], too. Also, obtained phase diagram shows significant difference comparing to the old version of AuIn-Sb phase diagram given by Prince et al. [7], who determined presence of simple eutectic reaction in the investigated section of the Au-In-Sb system. As Liu et al. [9] already determined, AuIn-Sb can not compose pseudobinary system, because when AuIn and Sb combine, reactions must happen when annealed.

Further characterization of the investigated alloys in the Au-In-Sb system, have been done using SEM-EDX, optic microscopy, hardness and electrical conductivity measurements.

The results of SEM analysis are presented in Fig.2, while characteristic microphotographs recorded by optic microscopy are given in Fig.3. Light phase, presented in following figures corresponds to AuIn, while dark phase is antimony-based, as confirmed by EDX analysis results given in Table 3.

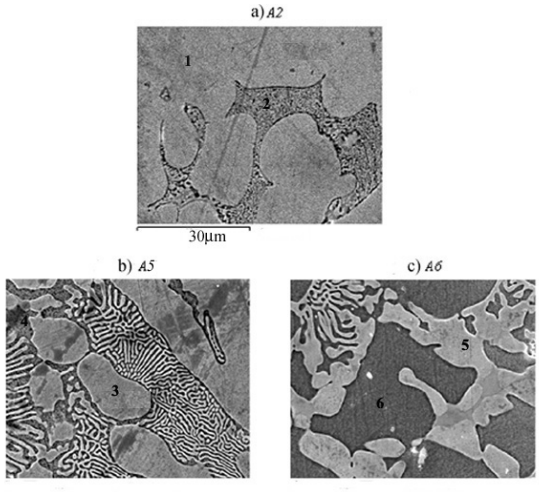

Fig.2. SEM microphotographs for the samples A2 (a), A5 (b) and A6 (c).

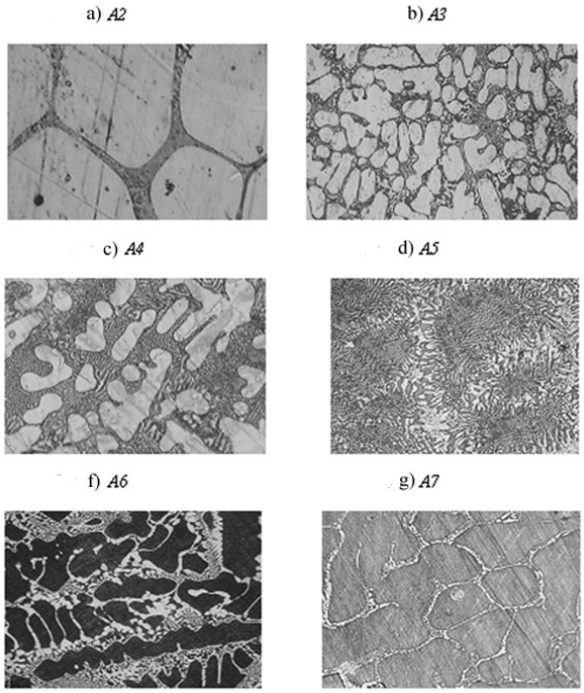

Fig.3. Characteristic optical microphotographs for: a) A2, b) A3, c) A4, d) A5, e) A6, f) A7

Table 3. The results of EDX analysis for the samples A2, A5 and A6.

Sample	Phase (in Fig.1)	Experimental composition		
		at% Au	at% In	at% Sb
A2	1	55.4	44.6	/
	2	59.31	23.74	16.95
A5	3	53.97	46.03	/
	4	2.37	/	97.63
A6	5	55.46	44.54	/
	6	/	/	100

The results of hardness measurements are shown in Table 4 in Fig.4. Hardness shows maximum peak at a concentration of x_{Sb} = 0.05, while in the concentration range over this composition hardness decreases as antimony content increases.

Table 4. The results of hardness measurements.

Alloy	x_{Sb}	HV5
A1	0	99.4
A2	0.05	126
A3	0.2	94.7
A4	0.28	89.13
A5	0.4	94.57
A6	0.65	79.93
A7	0.85	57.77

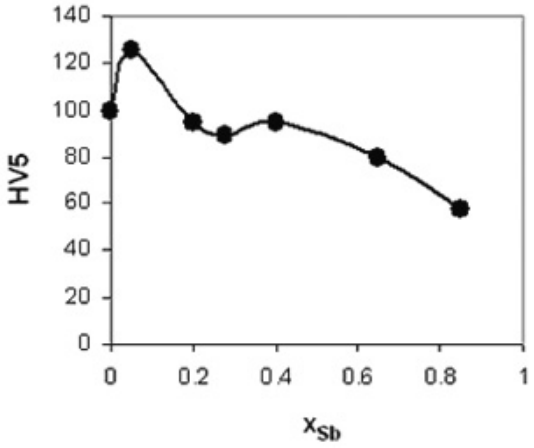

Fig. 4 Hardness vs. composition.

The results of electrical conductivity measurements are presented in Table 5, for three measuring series, and in Fig.5, where electrical conductivity dependence on composition is showed. As can be seen, the electrical conductivity decreases rapidly with antimony concentration increase in the investigated alloys.

Table 5. Measured values of electrical conductivity for investigated Au-In-Sb alloys

Alloy	Electrical conductivity (MS/m)		
A1	12.94	12.77	12.99
A2	7.396	7.546	7.339
A3	5.660	5.664	5.572
A4	5.533	5.522	5.536
A5	4.287	4.283	4.268
A6	2.667	2.633	2.644
A7	0.5475	0.6700	0.4948

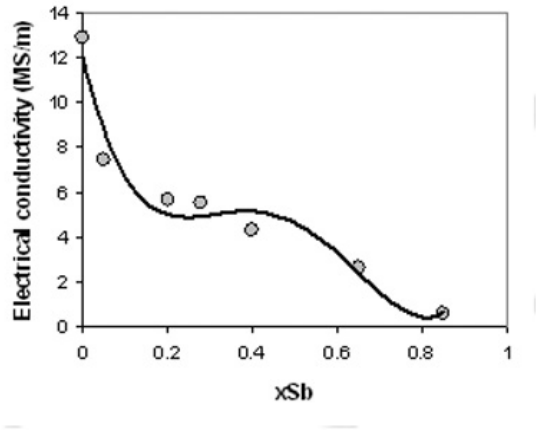

Fig.5. Electrical conductivity vs. composition

4. Conclusions

Phase diagram of the AuIn-Sb section in ternary Au-In-Sb system has been calculated by thermodynamic modeling based on constitutive binary systems data using ThermoCalc software, and confirmed by experimental results. The alloys chosen in section AuIn-Sb have been characterized using different experimental methods - DTA, SEM-EDX, optic microscopy, hardness and electrical conductivity measurements. Measured values of hardness and electrical conductivity show rapid decrease by antimony content increase in the investigated alloys.

Acknowledgement

This work was supported by Ministry of Science and Environmental Protection of the Republic of Serbia (Projects No. 142043 and 142035) and also, in the frame of the European action COST 531 on lead-free solder materials. Calculations were performed by ThermoCalc software.

References

[1] S. Rapsow, T. Groegewald, Gold Usage, Academic Press, London, 1978.
[2] J. S. Hwang, Environment-friendly electronics: Lead-free technology, Electrochemical Publications Ltd., Port Erin 2001, pp.97.
[3] http://www.patentstorm.us/patents/6312780-description.html
[4] http://www.freepatentsonline.com/6022605.html
[5] R. Kubiak, K. Schubert, Z. Metallkd. **71**, 635 (19800.
[6] C. T. Tsai, R. S. Williams, J. Mater. Res. **1**, 352 (1986)
[7] A. Prince, G. V. Raynor, D. S. Evans, Phase Diagrams of Ternary Gold Alloys, The Institute of Metals, London 1990, pp.295.
[8] W.E. Liu, S.E. Mohney, Materials Science and Engineering **B103**, 189 (2003).
[9] H. S. Liu, C. L. Liu, C. Wang, Z. P. Jin, K. Ishida, J. Electron. Mater. **32**, 81 (2003).
[10] http: //www.ap.univie.ac.at/users/www.cost531
[11] A. T. Dinsdale, A. Kroupa, J. Vízdal, J. Vrestal, A. Watson, A. Zemanova, COST531 Database for Lead-free Solders, Ver. 2.0, (2006), unpublished research.
[12] N. Saunders, P. Miodownik, CALPHAD (CALculation of PHAse Diagrams): A comprehensive guide, Pergamon, New York 1998.
[13] H.S. Liu et al., Calphad **27**, 27 (2003).
[14] E. Zoro et al., J.Phase Equilib.Diffus. **28**(3), 250. 2007
[15] T. Anderson et al., Calphad, **18**(2), 177 (1994).

APPENDIX:

OPTIMIZED THERMODYNAMIC PARAMETERS FOR CONSTITUTIVE BINARIES USED FOR CALCULATION

LIQUID
CONSTITUENTS: AU,IN,SB

L(LIQUID,AU,IN;0) = -76196.19+64.2914*T-6.6375*T*LN(T) [13]
L(LIQUID,AU,IN;1) = -31134.02+81.3582*T-8.5134*T*LN(T) [13]
L(LIQUID,AU,SB;0) = -10288.0428-14.7865028*T [14]
L(LIQUID,AU,SB;1) = -2901.66787-7.2503632*T [14]
L(LIQUID,AU,SB;2) = +1217.43604-4.74909763*T [14]
L(LIQUID,IN,SB;0) = -25631.2+102.9324*T-13.45816*T*LN(T) [15]
L(LIQUID,IN,SB;1) = -2115.4-1.31907*T [15]
L(LIQUID,IN,SB;2) = 2908.9 [15]

FCC_A1
2 SUBLATTICES, SITES 1: 1
CONSTITUENTS: AU,IN,SB : VA

L(FCC_A1,AU,IN:VA;0) = -48493.65+46.6237*T-6.8308*T*LN(T) [13]
L(FCC_A1,AU,IN:VA;1) = 498.45
L(FCC_A1,AU,SB:VA;0) = +31456.5511-35.1097911*T [14]
L(FCC_A1,IN,SB:VA;0) = -20000+15*T

RHOMBOHEDRAL_A7
EXCESS MODEL IS REDLICH-KISTER_MUGGIANU
CONSTITUENTS: IN,SB

L(RHOMBOHEDRAL_A7,IN,SB;0) = 298.14<T< 1000.00: +15*T [11]

AUSB2
2 SUBLATTICES, SITES 0.333333: 0.666667
CONSTITUENTS: AU : IN,SB

G(AUSB2,AU:IN;0)-0.333333 H298(FCC_A1,AU;0)-0.666667
H298(TETRAGONAL_A6,IN;0) =
+5000-
2*T+.333333*GHSERAU+.666667*GHSERIN
G(AUSB2,AU:SB;0)-0.333333 H298(FCC_A1,AU;0)-0.666667
H298(RHOMBOHEDRAL_A7,SB;0) =
-5721.66949+6.93505837*T-.62*T*LN(T) [14]
+0.333333*GHSERAU+0.666667*GHSERSB
L(AUSB2,AU:IN,SB;0) = -5000

TETRAGONAL_A6
CONSTITUENTS: IN

AU3IN
2 SUBLATTICES, SITES 0.75: 0 .25
CONSTITUENTS: AU : IN

G(AU3IN,AU:IN;0)-0.75 H298(FCC_A1,AU;0)-0.25 H298(TETRAGONAL_A6,IN;0) =-10582.67-2.9323*T+.75*GHSERAU+.25*GHSERIN [13]

AU7IN3
2 SUBLATTICES, SITES 0 .7: 0.3
CONSTITUENTS: AU : IN

G(AU7IN3,AU:IN;0)-0.7 H298(FCC_A1,AU;0)-0.3 H298(TETRAGONAL_A6,IN;0) =
-12813.11-2.0538*T+.7*GHSERAU+.3*GHSERIN [13]

AUIN
2 SUBLATTICES, SITES 0.5: 0 .5
CONSTITUENTS: AU : IN,SB

G(AUIN,AU:IN;0)-0.5 H298(FCC_A1,AU;0)-0.5 H298(TETRAGONAL_A6,IN;0) =
-20188.37+2.3786*T+.5*GHSERAU+.5*GHSERIN [13]
G(AUIN,AU:SB;0)-0.5 H298(FCC_A1,AU;0)-0.5H298(RHOMBOHEDRAL_A7,SB;0) =+6000-3*T+.5*GHSERAU+.5*GHSERSB
L(AUIN,AU:IN,SB;0) = -4000

AUIN2
2 SUBLATTICES, SITES 0.333333: 0.666667
CONSTITUENTS: AU : IN,SB

G(AUIN2,AU:IN;0)-0.333333 H298(FCC_A1,AU;0)-0.666667
H298(TETRAGONAL_A6,IN;0) = -26129.06+11.1133*T+0.333333*GHSERAU
+0.666667*GHSERIN
G(AUIN2,AU:SB;0)-0.333333 H298(FCC_A1,AU;0)-0.666667
H298(RHOMBOHEDRAL_A7,SB;0) = +8000-T+.333333*GHSERAU
+0.666667*GHSERSB
L(AUIN2,AU:IN,SB;0) = -3000 [11]

AUIN_ALPHA1
EXCESS MODEL IS REDLICH-KISTER_MUGGIANU
CONSTITUENTS: AU,IN

G(AUIN_ALPHA1,AU;0)-H298(FCC_A1,AU;0) = +125+.79*T+GHSERAU
G(AUIN_ALPHA1,IN;0)-H298(TETRAGONAL_A6,IN;0) = +520-.384*T+GHSERIN
L(AUIN_ALPHA1,AU,IN;0) = -48238.66+5.3551*T [13]
L(AUIN_ALPHA1,AU,IN;1) = -48.36-16.7932*T

HCP_A3
2 SUBLATTICES, SITES 1: .5
CONSTITUENTS: AU,IN,SB : VA

L(HCP_A3,AU,IN:VA;0) = -55780.55+13.8198*T [13]
L(HCP_A3,AU,IN:VA;1) = +6788.95-32.8937*T [13]
L(HCP_A3,AU,SB:VA;0) = 298.14<T< 1000.00: 7580
L(HCP_A3,IN,SB:VA;0) = 298.14<T< 1000.00: -20000+15*T

AUIN2

L(AUIN2, AU:IN,SB,0) = -3000 [9]

AUIN_BETA
2 SUBLATTICES, SITES 0.785: 0.215
CONSTITUENTS: AU : IN

G(AUIN_BETA,AU:IN;0)-0.785 H298(FCC_A1,AU;0)-0.215 H298(TETRAGONAL_A6,IN;0) = -8980.42-3.3042*T+.785*GHSERAU+.215*GHSERIN [13]

AUIN_BETAP
2 SUBLATTICES, SITES 0.77778: 0.22222
CONSTITUENTS: AU : IN

G(AUIN_BETAP,AU:IN;0)-0.77778 H298(FCC_A1,AU;0)-0.22222
H298(TETRAGONAL_A6,IN;0) = -9382.52-3.1015*T+0.77778*GHSERAU
+0.22222*GHSERIN [13]

AUIN_PSI
3 SUBLATTICES, SITES .5: 0.33333: 0.16667
CONSTITUENTS: AU : AU,IN : IN

G(AUIN_PSI,AU:AU:IN;0)-0.83333 H298(FCC_A1,AU;0)-0.16667

H298(TETRAGONAL_A6,IN;0) = +2153.38-
8.039*T+.83333*GHSERAU
+0.16667*GHSERIN [13]
G(AUIN_PSI,AU:IN:IN;0)-0.5 H298(FCC_A1,AU;0)-0.5
H298(TETRAGONAL_A6,IN;0) = -
18225.14+3*T+.5*GHSERAU+.5*GHSERIN [13]
L(AUIN_PSI,AU:AU,IN:IN;0) = -15683.16 [13]

AUIN_GAMMA
3 SUBLATTICES, SITES 0.69231: 0.23077: 0.07692
CONSTITUENTS: AU : AU,IN : IN

G(AUIN_GAMMA,AU:AU:IN;0)-0.92308
H298(FCC_A1,AU;0)-0.07692
H298(TETRAGONAL_A6,IN;0) = -2830.47-
2.5191*T+0.92308*GHSERAU
+0.07692*GHSERIN [13]
G(AUIN_GAMMA,AU:IN:IN;0)-0.69231
H298(FCC_A1,AU;0)-0.30769
H298(TETRAGONAL_A6,IN;0) = -11992.16-
3.6511*T+0.69231*GHSERAU
+0.30769*GHSERIN [13]
L(AUIN_GAMMA,AU:AU,IN:IN;0) = 2144.6 [13]

ZINCBLENDE_B3
2 SUBLATTICES, SITES 0.5: 0.5
CONSTITUENTS: IN : SB

G(ZINCBLENDE_B3,IN:SB;0)-0.5
H298(TETRAGONAL_A6,IN;0)-0.5
H298(RHOMBOHEDRAL_A7,SB;0) =-
16411.1+.81674*T+1.293581*T*LN(T)
+0.5*GHSERIN+0.5*GHSERSB [11]

*Contact person: dzivkovic@tf.bor.ac.yu